*i*Journals: International Journal of Social Relevance & Concern (IJSRC)
ISSN-2347-9698
Volume 11 Issue 11 November 2023

The use of Landsat 8 OLI image for the delineation Hydrothermal Alterations Zones in the Haiya Area, Red Sea Hills, NE Sudan

Authors: Adam Alsaid Blila Mohammed[1]; Sami Omer Hag El Khidir[2]

Affiliation: [1] Regional Geology Administration , Geological Research Authority of Sudan (GRAS), Ministry of Minerals ,Khartoum, 410 , Sudan; [2]Department of Geology, Faculty of Petroleum and Minerals , Al Neelain University, 52ndSt , Khartoum, 12702, Sudan

E-mail: [1] adamalsaid9@gmail.com; [2]sami.elkhidir@gmail.com

DOI: 10.26821/IJSRC.11.11.2023.111102

ABSTRACT

Remote Sensing and GIS investigations were carried out in the area around Haiya- Tohamiyam town in the Red Sea Hills, NE Sudan. The study aimed to delineate the alteration zones-related to mineralizations. The optical multispectral Landsat 8 OLI utilized remotely sensed data. The study area is a part of Haiya terrane (HT) of the late Proterozoic Arabian- Nubian Shield (ANS). The Haiya terrane consists predominantly of arc- back arc low-grade metavolcanosedimentary sequences decorated with dismembered ophiolitic rocks and intruded by granitoids intrusions of different age. The band ratios FCC images of Sabins' (6/7, 4/6 and 4/2 in R, G & B), and Abram's (6/7-6/5-4/2 in R, G & B), delineate the alteration zones in the study area. The obtained results authenticated by the Feature Oriented Principal Components (FOPCT) results of the two sets for F- and H- images. The FCC image known as Crosta's alteration zones image (F-image, {F + H image}, H-image in the R, G and B respectively). The image transformations revealed that the alteration zones are associated with the basic metavolcanics and exo-endo contacts of the post orogenic granites with other metavolcanics.

Keywords: Landsat 8, Hydrothermal Alterations zones, Haiya Area, Red Sea Hills, Sudan.

1. INTRODUCTION

The Red Sea Hills (RSH) is an extending regional topographic feature in Egypt, Sudan, Eretria, Ethiopia, Saudi Arabia and Yemen. The RSH formed as result of the late Proterozoic East African Orogen, latter split by rifting and formation of the Red Sea. The RSH have been well known as one potential mineralization terrane. In particular, in the Sudan the existence of mineral deposits such as gold, copper, iron and other associate minerals of economic values recorded in this mountainous terrain. The rigidness topography, harsh environment and lack of good infrastructure in the RSH hindered the development of mining industry. The development of any region started by the well and sustainable utilization of the natural resources. The systematic development plans in any region involve systematic prospecting and exploration programs to utilize the natural resources in a sustainable manner. Hence, the remote sensing as science, techniques and methodologies proved to be a valuable for many geological fields, specifically the regional geological mapping, prospecting and exploration of the suitable mineral deposits and water resources. In Sudan many researches involve the optical and radar remote sensing data have been conducted for geological mapping and mineral exploration [1]; [2]; [3]; [4]; [5]; [6]; and [7].

The study area lies around Tohamiyam town and railway Station in the Red Sea Hills. Administratively, the area lies within the boundaries of the Sinkat and Haiya localities in the Red Sea State. Geographically, the area under consideration is mapped within the Sinkat topo-sheet (NE-37-E-Sinkat; scale 250K), bounded by longitudes 36° 10' 35.4" E- 36° 53' 7.4" E, and latitudes 18° 46' 46.4" N- 18° 14' 25" N. The main towns in the study area are Haiya, Tohamiyam and

Summit "Fig. 1". Haiya town lies in the junction of two highways of the can be accessed via the national highway network, which connects Khartoum (Sudan capital) and Port Sudan (The main port). Therefore, the area can be access by the main national highway road connects Khartoum- Atbara- Haiya- Port Sudan (800-Km), while the second national highway road connects Khartoum-Wad Medani- Gedarif- Kassala- Haiya- Port Sudan (1200-Km). The railway runs parallel to first highway road. Regular daily flights are running between Khartoum-Port Sudan.

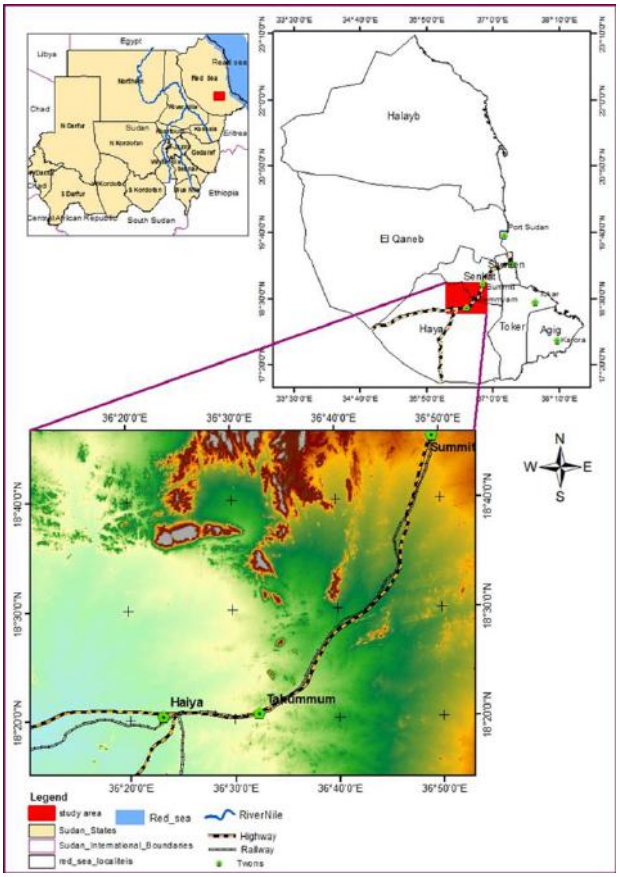

Fig. (1): Location map of the study area.

2. GEOLOGY AND TECTONIC SETTING

The Red Sea Hills "RSH" represent the western part of the Arabian- Nubian Shield "ANS", which dominated by arc and back arc metavolcanosedimentary sequences decorated by mafic ultramafic ophiolitic sutures formed by Pan African orogeny in the Neoproterozoic age [8]. The Sudanese RSH region occupies a central position in the Nubian segment of the ANS. These hills constitute a semi desert plateau of mountains no more than 200-Km wide and rising up to 2000-m (*a. m. s. l.*). The mafic- ultramafic ophiolite complexes represent suture zones along which oceans and back- arc basins have closed [9]; [10] and were probably continuous with their equivalents on the Arabian side of the ANS [11]; [12]; and [13]. The geological studies in NE Sudan started since the early 1950s, in 1976, Vail attempted to integrate the Red Sea Hills into the geology of the entire ANS [14]. Further subsequent work led to a first evolutionary model for the region, whereby three separate crustal entities were identified, each reflecting temporally distinct cycles of magmatic activity separated by ophiolite belts [10]; [11]. Others supported the arc accretion model developed for the Eastern Desert of Egypt and Western Arabia, on the basis of remarkable similarity of rock types and their tectonic setting with those of NE Sudan [15]. This region has been correlated with adjacent areas in NE Africa and divided into two major geodynamic systems, namely gneisses with interfolded supracrustal metasediments and a dominantly low-grade juvenile ophiolitic island-arc assemblage [16]. The Precambrian basement complex of RSH is divided three major lithological units; these three lithological units are:

1) High- grade gneisses, formerly known as (Kashabib series), representing the roots of the arc assemblages.
2) Low- grade volcanosedimentary sequence, formerly named (Nafirdeib Series).

3) A more differentiated, less metamorphosed volcanosedimentary sequence, formerly known as (Awat Series). These lithological units were extensively intruded by plutonic rocks, emplaced at different times during the tectonomagmatic history of the basement complex of the Red Sea Hills [17]; [18].

The igneous intrusive rocks cover about 50% of the total area of the RSH terrains. They vary in mode of occurrence from huge batholiths to stocks and plugs, whereas. ring complexes and dyke swarms are common. Intrusive of the RSH terrains emplaced at different times during the Pan-African orogeny. Accordingly, they have been classified as syn- to late- and post- orogenic granitoids or intrusions [19]. The Nubian Shield is dominated by volcanogenic sediments metamorphosed in greenschist facies. These rocks comprise arc volcanics and associated intrusive rocks, immature sediments and ophiolitic remnants of arc- and back-arc basins [17; [18]. This shield itself divided into five intra oceanic and island-arc terranes, separated by sutures and shear zones, these five terranes, from north to south are Gerf, Gabgaba, Gebeit, Haiya and Tokar [20]; [21].

3. METHODOLOGY

The present investigations based on the digital image processing and of the multispectral remotely sensed data, combined with GIS spatial analysis and cartography manipulation, a very few field work data have been manipulated within the course of the study.

3.1 The Optical Multispectral Landsat 8 OLI data

The American Landsat series is one of the famous and worldwide Earth Observation System (EOS) providing free data. Landsat 8 is the eighth satellite in the Landsat program, launched on February 11th, 2013. It's the seventh to reach orbit successfully. Originally, called the Landsat Data Continuity Mission (LDCM), it is a collaboration between NASA and the United States Geological Survey (USGS). The system was later change to OLI (Operational Land Imager).Landsat 8 satellite is Pushbroom platform, sun synchronous, sub polar orbit with altitude 705 Km and revisiting time 16 days. Landsat 8 ensures the continued acquisition and availability of Landsat data utilizing a two- sensor payload: The Operational Land Imager (OLI) and the Thermal InfraRed Sensor (TIRS), respectively (http://landsat.usgs.gov). These two instruments collect image data for nine shortwave bands and two long wave thermal Bands.

The spectral bands of Landsat 8 Oli are well-suited for recognizing assemblages of alteration minerals (iron oxides, clay, and alunite) that occur in hydrothermally altered rocks. The OLI was designed to detect the same spectral bands as earlier Landsat instruments with the exception of the thermal infrared band "Table 1".

Table (1):Landsat 8 OLI and TIRS Spectral Bands

Band	Spectral rang (µm)	Spatial resolution (m)
Band 1- coastal	0.43-0.45	30
Band 2- blue	0.45-0.51	
Band 3- green	0.53-0.59	
Band 4- red	0.64-0.67	
Band 5- Near IR	0.85-0.88	
Band 6- SWIR 1	1.57-1.65	
Band 7- SWIR -1	2.11-2.29	
Band 8- Panchromatic	0.50-0.68	15
Band 9- cirrus	1.36-1.38	100
Band 10- TIR 1	10.30-11.30	
Band 11- TIR 2	11.50-12.51	

Single scene of Landsat 8 OLI data has been downloaded from USGS official web site (www:// earth explorer.org), as separate files as GeoTiff format as cover the study area was used, which is defined as:

• LC08_L1TP_171047_20180915_20180928_01_T1, acquisition date: February 9th , 2018.

3.2 Digital Image Processing

The Fast Line-of-sight Atmospheric Analysis of Hypercubes (FLAASH) algorithm was applied for atmospheric correction for the Landsat 8 OLI data as the main preprocessing operation. Whereas the main digital image processing operations are image transformation operations. Moreover, The GIS Geodatabase enables the geo-spatial analysis to establish the results. The best exploration results are obtained by combining geologic and fracture mapping with the recognition of hydrothermally altered rocks. A variety of remote sensing tools is now available to the exploration geologists. Accordingly, the present study will rely largely on the interpretation of Landsat 8 OLI image, whereby the alterations zones can be accurately mapped utilizing the band ratioing techniques which is capable of emphasizing alteration zones. Band ratioing technique has been proved powerful in discriminating (being rich in iron oxides) from the rest of the country rocks. Geochemical analysis was conducted for a number of samples, collected during the field work.

4. RESULTS AND DISCUSSIONS

4.1 Digital image Processing of Landsat 8 OLI

One of the main objectives of this study is to delineate the hydrothermal alteration zones associated with porphyry copper mineralization and related host rocks. The porphyry copper mineralization has been discovered in many areas in the RSH. Image transformations approach, namely band ratio and feature oriented principal component analysis were used for mapping the hydrothermally altered zones – related to mineralizations. The band rationing is a well-known method in geologic remote sensing. Band ratio transformation is useful for qualitative detection of hydrothermal alteration clay minerals and iron oxides. The band ratio image of Landsat 8 OLI (band 4/band 2), which indicate the (Red band /Blue band) is well known to delineate iron oxide rich zones in brighter tones, as the iron oxides have high and low reflectance in the red and blue spectrum, respectively. The band ratio image of Landsat 8 OLI (band 6/band 7), portray the band ratio of (SWIR 1 band /SWIR 2 band) is well known to depict the hydroxyl-bearing minerals and specifically the clay minerals in the alteration zones in brighter tone due to the major absorption bands of all hydroxyl- bearing and clay minerals in the SWIR 2 spectrum.

The ratio image of Landsat 8 OLI band 4/band 2 revealed the iron oxides rich areas in brighter tone, however, the density slicing enhancement revealed better discernable image as the high values appear in red and lowest values appear in blue hues. The band ratio image displays the areas rich in iron oxides mainly in the eastern parts of the study area. Moreover, the alluvial wadies display in brighter tones indicating the richness of wadies by the weathering products of the iron minerals “Fig. 2 a & b”.

The ratio image of band 6/band 7 revealed the areas rich in hydroxyl- bearing minerals and specifically the clay minerals (for example, montmorillonite, illite, kaolinite and alunite). The areas rich in clay minerals and associated hydroxyl-bearing minerals appear in brighter tone, however, the density slicing enhancement revealed better discernable image as the high values appear in red and lowest values appear in blue hues. The resultant images display areas rich in clay minerals in the central upper region of the study associated with the metavolcanosedimentary sequences and related granitoid. “Fig. 2 c & d”.

The color composite image has been created by selecting different band ratio images such as above and others in the R, G and B color gun spectrum. In this context, two well-known FCC band ratio images have been created to delineate and map the alteration zones related to mineralization, which are named as Abram’s and Sabins’ FCC band ratio images.

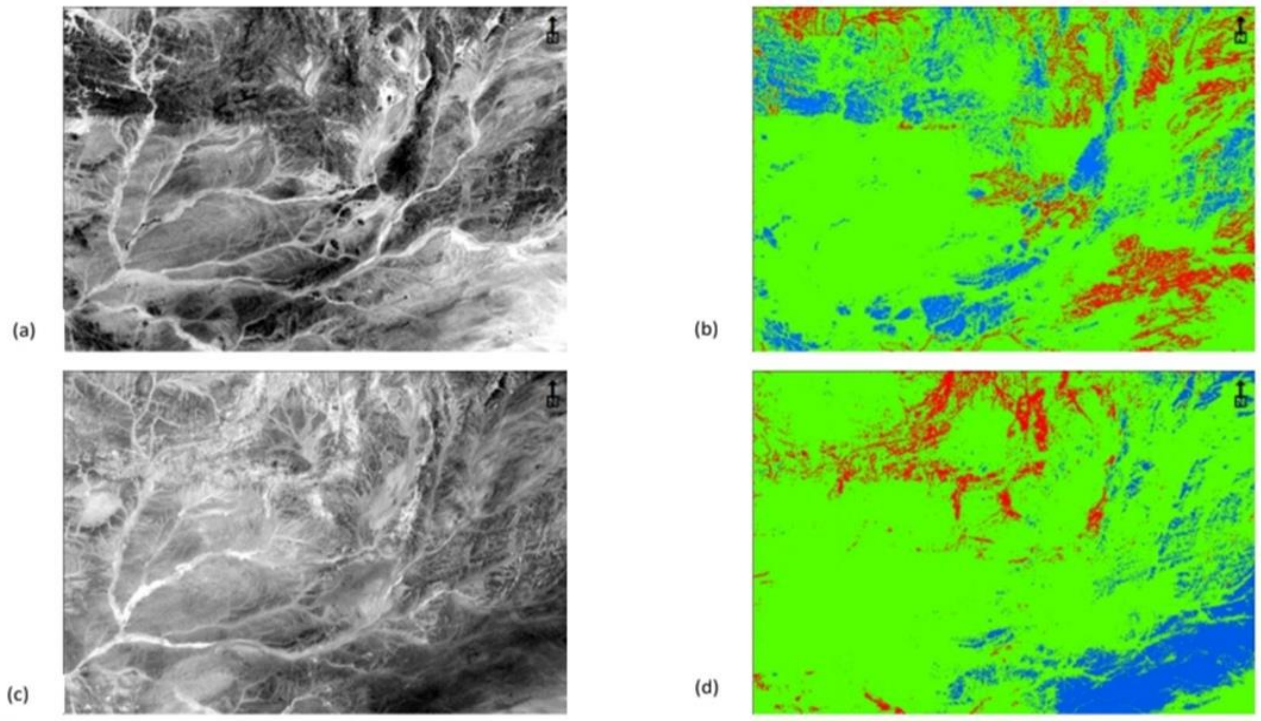

Fig. (2): (a) Gray scale image of band ratio image of band (4/ 2) displays iron oxide in (bright) color. (b) Density Slicing Image of band ratio image of band (4/ 2) for iron oxide (Red is highest values). (c) Gray scale of band ratio image of band ratio (6/ 7) displays clay and hydroxyl bearing minerals in (bright color). (d) Density Slicing Image of band ratio (6/ 7) for clay and hydroxyl bearing minerals (Red is highest values).

The Abram's band ratioing FCC image produce by selecting the band ratio images of Landsat 8 OLI data of band ratios (6/7), (6/5), and (4/2) in the R, G and B, respectively [22]. The Abram's FCC image displays alteration zones related to the mineralization in bright yellowish hues, normally buffered by reddish hues. Most granitoids areas appear in blueish hues, while the metavolcanosedimentary sequences display green and red hues according to their composition. The wadies' alluvial deposits display violet and blue hues "Fig. 3".

However, the Sabins' band ratio FCC image produce by selecting the band ratio images of Landsat 8 OLI data of band ratio (6/7), (4/2), and (4/6) in the R, G and B, respectively [23]. The Sabins FCC image is better than the Abram's one in depicting the alteration zones and other lithological units. In this image the alteration zones related to the mineralization are display in spectacular crimson reddish hues, which appear as lenses and patches within the metavolcanics. Most granitoids areas appear in greenish hues, while the metavolcanosedimentary sequences display green and navy-blue hues according to their composition. The wadies' alluvial deposits display cyanic hues "Fig. 4".

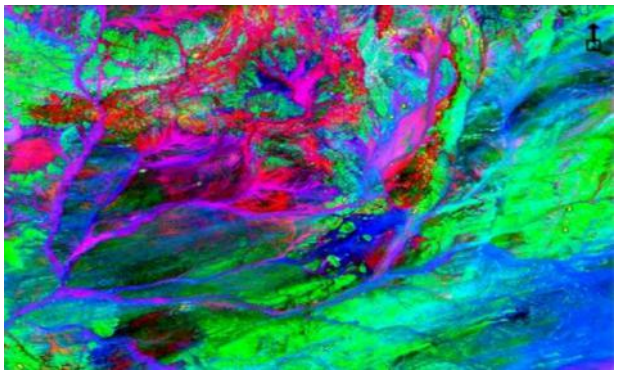

Fig. (3): FCC Abram's band ratio FCC image of Landsat 8 OLI data of band ratios (6/7), (6/5), and (4/2) in the R, G and B, respectively. The obtained the alteration zones depicted in bright yellowish hues (after Abram, et al. 1983).

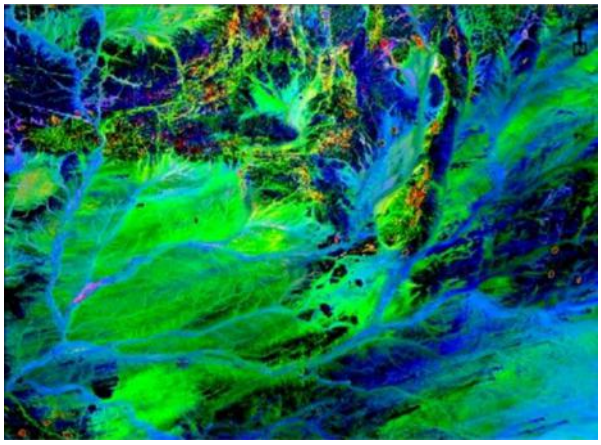

Fig. (4): FCC Sabins' band ratio image of Landsat 8 OLI data of band ratio (6/7), (4/2), and (4/6) in the R, G & B, respectively. The image depicting alteration zones in crimson reddish hues (after Sabins, 2000).

The Feature-Oriented Principal Component Selection (FOPCS). This method was developed with the purpose of using remote sensing satellite images for geologic exploration in an environment lacking bedrock exposure, and is well-known as Crosta Alteration zones image. Selected bands believed to contain spectral information over an intended target are used in PCA transformation for enhancement of two sets of four bands. The PCA method is known as Feature Oriented Principal Selection technique (FPCS) by selecting two sets are bands 2, 3, 4, & 5 for delineating the iron oxides rich areas and known as (F- image), the other set are bands 4, 5, 6 and 7 and used to delineate areas rich in clay minerals and known as (H-image). This selection is based on the fact that the former has contrasting signatures in bands (2 & 4) and the latter bands (6 & 7) in Landsat 8 OLI. The image defines alteration zones usually in terms of their iron oxides and clay minerals richer zones "Tables 2 and 3". From the two tables clearly indicate that the PC3 in both transformations contain bigger arithmetic differences. However, both PC3s contain negative values in the band which should be as nominator while the values of the dominator bands are positive, which involve image negation processes before using as a guide image and then applying median filter as low-pass filter to remove the small noises to reveal the areas rich in iron oxides and clay minerals in brighter tones or red hues in the gray scale and density slices images, respectively "Fig. 5". The FCC Crosta image produced by combining the H-image, (H-image+ F-image), and F-image in the R, G, and B color gun to depicting the potential alteration zones in white, yellowish and golden hues "Fig. 6".

Table (2): The eigenvectors loading for F- image

Eigen-vector	Band 2	Band 3	Band 4	Band 5
PC1	0.275848	0.436442	0.586215	0.624322
PC2	0.583981	0.466063	0.080814	-0.659713
PC3	0.606348	-0.060412	-0.678063	0.411002
PC4	-0.463914	0.767238	-0.435949	0.077963

Table (3): The eigenvectors loading for H- image

Eigen-vector	Band 4	Band 5	Band 6	Band 7
PC1	450151	0.483299	0.537768	0.524015
PC2	0.502808	0.516055	-0.257125	-0.644018
PC3	0.551400	-0.292476	-0.638060	0.450882
PC4	-0.490414	0.643869	-0.487412	0.327652

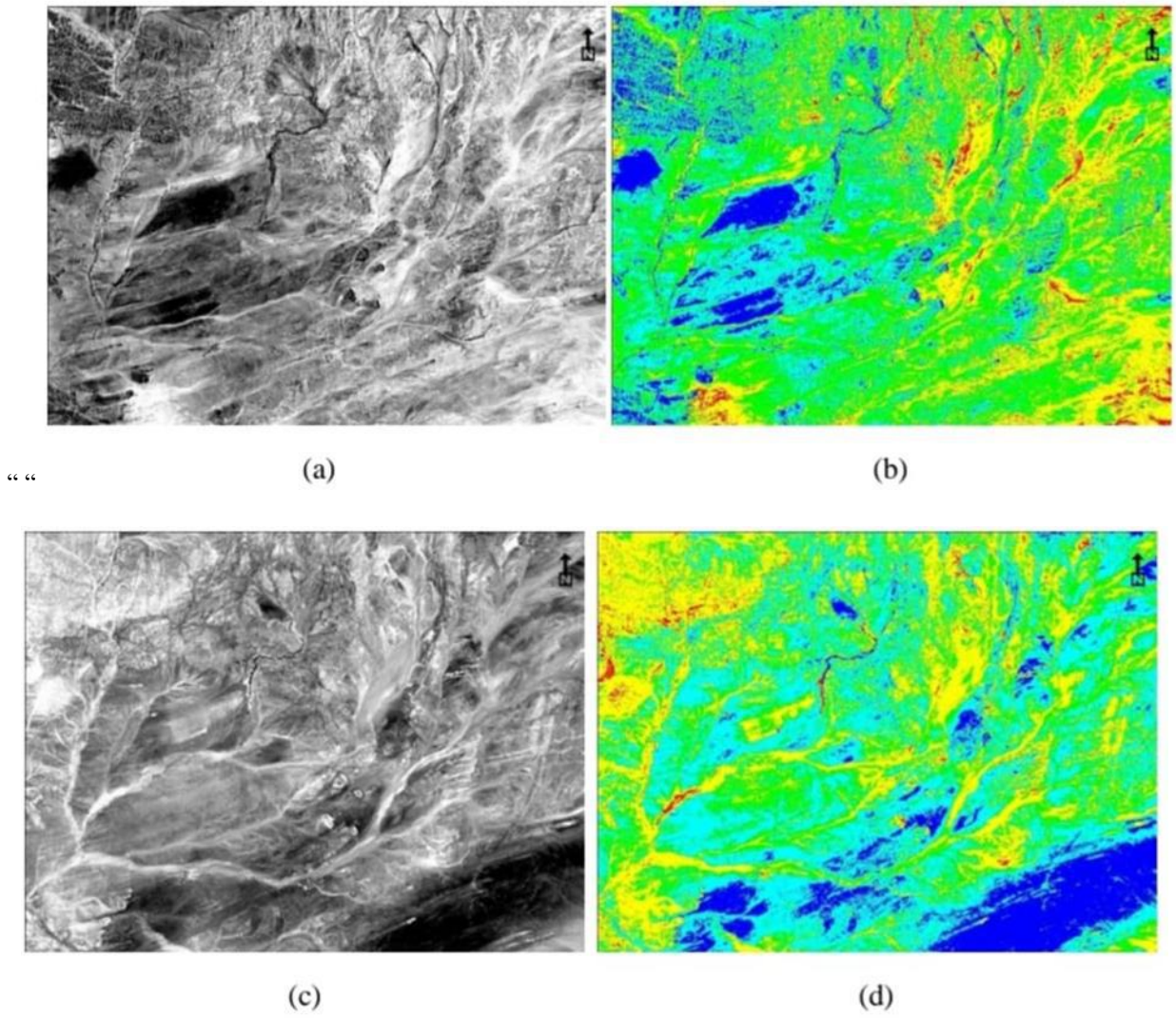

Fig. (5): Result images of the FPCS analysis for selected F- & H- images (a) Gray –scale of F-image depicting high values in bright tones. (b) Density slicing of F-image depicting high values in red color. (c): Gray –scale of H-image depicting high values in bright tones. (d) Density slicing of H-image depicting high values in red color.

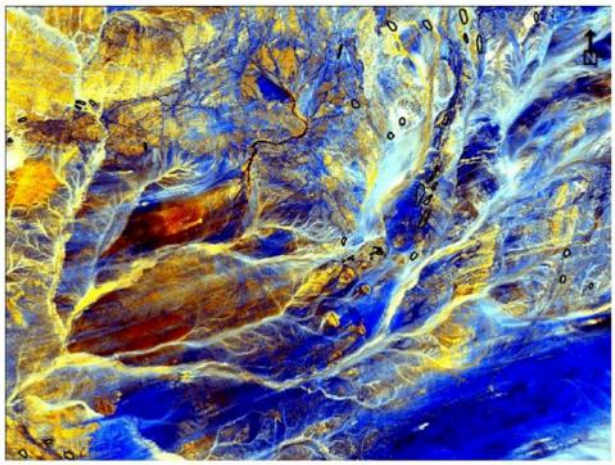

Fig. (6): Crosta FCC image produced from the FPCS products to revealed the alteration zones related to mineralization. FCC image produced by selection of {H-images}, {H image + F image}, {F-image} in the R, G and B, respectively. The depicted alteration zones-related to mineralization depicting in white-yellowish and golden hues.

4.2 Geochemical Analysis

Based on the results of OLI image interpretation, 14 alteration zones samples to delineation hydrothermally altered rocks located by global position system (GPS). Alterations samples were selected for XRF analysis from the delineated porphyry copper. The obtained results are displayed in "Table 4". However, more accurate analytical technique Atomic Absorption Spectrometry (AAS) are recommended. These samples were taken from different areas from Haya area, the samples were taken analyzed in laboratory of the Geological Research Authority of Sudan (GRAS)." "**Table(4). Chemical analysis for trace elements of the study area**

Sample No.	Au (ppm)	Ag (ppm)	Pb (ppm)	Cu (ppm)	Co (ppm)	Zn (ppm)	Ni (ppm)	Mn (ppm)	Cr (ppm)
HRS1A	0.022	0.9	14.7	36.6	6.2	56.1	8.2	4.367	27.7
HRS3	0.048	20.0	15.3	33.5	17.8	96.5	28.4	11.415	78.2
HRS4A	0.179	2.9	21.9	8.1	16.4	88.1	44.2	9.710	124.9
HRS4B	0.129	1.1	26.8	471.0	9.9	45.1	38.8	10.506	135.8
HRS5B	0.253	15.3	16.9	51.5	8.1	59.9	32.1	9.974	98.0
HRS6	0.231	9.4	23.7	153.0	24.7	91.5	130.4	10.025	332.9
HRS8	0.113	1.4	21.5	179.3	12.8	121.9	15.9	9.833	116.6
HRS9	0.100	1.9	22.0	178.8	23.0	117.7	68.4	10.747	135.6
HRS11A	0.134	3.0	19.0	40.9	30.3	111.1	67.5	10.546	245.9
HRS11B	0.338	5.3	21.5	52.2	27.9	87.6	50.9	10.264	173.4
HRS12	0.121	3.2	26.4	57.3	35.5	121.5	88.1	12.900	144.4
HRS13	0.117	2.4	21.8	8.0	28.4	65.1	56.5	11.248	64.9
HRS14	0.114	2.4	9.8	64.0	ND	33.9	14.7	5.650	ND
HRS15	0.160	1.6	18.1	15.2	27.8	136.1	62.4	12.091	125.6

4.3 GIS Spatial Analysis for Alteration Zones Mapping

The output and results of the image transformation from the band ratio and FPCS are clearly that the alterations zones-related to mineralization can be distinguished by their spectral signatures. However, it's necessary to convert these alterations zones from the raster format into vector format to facilitate the spatial analysis. Hence, the depicted alteration zones from Abram's and Sabins' band ratio FCC images have been converted to vector layers. Moreover, the alteration zones of the Crosta's FCC image mapped and converted to vector polygon format. GIS spatial analysis operations have

been applied on the vectorized polygon format. Firstly, the intersection between vectorized results of Sabins' and Abram's band ratio FCC images. Secondly, the intersected results are intersected again with the polygon results of Crosta's FCC image. The final results provide good results of the alteration zones, which related to regional N-S shear zones in the basic metavolcanics in the northeastern part and the exo-endo contacts of the acidic to intermediated metavolcanics with anorogenic granites. should have good reparability between various lithological classes and the altered zone "Fig. 7".

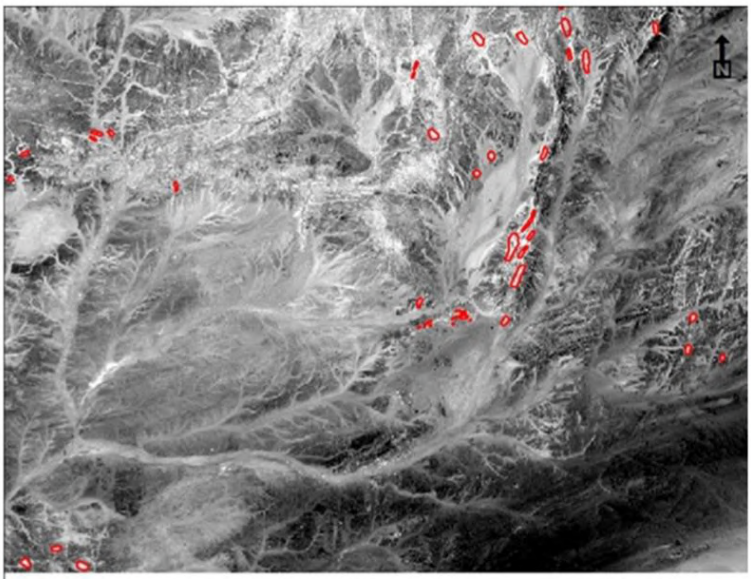

Fig. (7): Alteration map produced after the spatial analysis of the transformed images, overlay on the satellite imagery in red circles.

5. CONCLUSIONS

The study area is a part of the crystalline basemen of Haiya terrane of the late Proterozoic age. The area is dominated by low –grade arc- and back- arc metavolcanosedimentary sequences, which decorated by dismembered ophiolitic belts and intruded by granitoid intrusions of different ages. The Digital image processing revealed areas with favourable hydrothermal alteration signals that were later verified in the field. Geochemical analyses using portable XRF device and Atomic Absorption Spectrometry AAS analysis revealed the presence of alterations in the area. The outcome of the present study indicated high potentiality for alterations in the area. However, further detailed studies.

The band ratio image of landsat8 OLI is known to delineate the alteration zones by spectral signatures of iron oxides 4/2, clay minerals 6/7. Various FCC images of band ratio such as for Abrams' ratio (6/7, 6/5 and 4/2), Sabins' ratio (6/7, 4/6 and 4/2) were used to identify and delineate alteration zones. The demarcated alteration zones are potentially mapped on the basic metavolcanics.

Acknowledgments

The authors would like to many thanks to all teachers and colleagues of the M. Sc. Batch II: Applications of Remote Sensing and GIS in Geology for their valuable information, support and encourage during the course of my study, also to acknowledge my colleagues in Regional Geology Administration, Geological Research Authority of Sudan (GRAS) for their endless encourage and support. As well as, I would like to acknowledge the staff members of the Faculty of Petroleum and Minerals, Al Neelain University for their help and support. I would like to thank all friends and classmates who shared their words of advice and encouragement to finish this study.

References

[1]. I. A. A. Babikir, "Digital Image Processing of Landsat 7 data and GIS Application for Geological Investigation in Jebel Erba Area, Red Sea Hills, NE Sudan". Ph. D. thesis, Al Neelain University. Khartoum, Sudan. 2006.

[2] S. O. El Khidir, "Remote sensing and GIS applications in geological mapping, prospecting for mineral deposits and Groundwater-Berber sheet area, northern Sudan". Ph.D. thesis, Al Neelain University, Khartoum, Sudan. 2006.

[3] S. O. El Khidir and I. A. Babikir "Digital image processing and geospatial analysis of Landsat 7 ETM+ for mineral exploration, Abidiya area, North Sudan". International Journal of Geomatics and Geosciences. 2013. Vol. 3, No., 3, pp. 645- 658. ISSN 0976-4380.

[4] E, A. Ali, "The Geology and Structural Evolution of the Area around The River Nile Between Atbara and Abidiya, Nile State, Sudan: Remote Sensing, Structural and Geochemical Approaches". M. Sc. thesis, Al Neelain University, Sudan. 2005.

[5] K. A. Elsayed Zeinelabdein, "Application of remote sensing in geological mapping, hydrogeological investigation and mineral exploration, Red Sea Hills northeastern Sudan". M. Sc. Thesis. Dept. of Geology. U of K. Khartoum, Sudan. 2002.

[6] N. H. Kenea. Digital image processing and GIS data integration for geological studies in the Red Sea Hills, Sudan. Ph. D. Thesis. Free University of Berlin. Germany. 1997.

[7] M. G. Abdelsalam, R. J. Stern, H. Schandelmeier, and M. Sultan, "Deformational history of the Keraf Zone in NE Sudan, revealed by Shuttle Imaging Radar". Jour. Geology, v. 103. 1995. pp. 475–491.

[8] J. R. Vail, "Outline of geology and mineralization of the Nubian Shield east of the Nile Valley, Sudan". In: TAHON, S. A. (ed.), Evolution and mineralization of the Arabian-Nubian Shield, Proceed. Symp. 2. 1979. pp. 97-107, Oxford (Pergamon Press).

[9] W. R. Fitches, R. H. Graham, I. M. Hussein, A. C. Ries, R. M. Shackleton, and R. C. Price, "The Late Proterozoic ophiolite of the Sol Hamid, NE Sudan". Precam. Res., 19. 1983. pp. 385-411.

[10] J. R. Vail, "Pan - African crustal accretion in North – East Africa". Journal of African Earth Science, 1(3-4). 1983. pp. 285-294, Oxford.

[11] Vail, J. R. (1985): Pan - African (late Precambrian) tectonic terrains and the reconstruction of the Arabian- Nubian shield. Geology, 13, pp. 839-842, Boulder.

[12] V. E. Camp, "Island arcs and their role in the evolution of the western Arabian Shield". Geol. Soc. Am. Bull., 95. 1984. Pp. 913-921, Washington.

[13] A. R. Bakor, I. G. Gass, and C. R. Neary, "Jabal al Wask, northwest Saudi Arabia: An Eocambrian back-arc ophiolite". Earth and Planetary Science Letters, 30. 1976. pp. 1-9.

[14] J. R. Vail, "Outline of the geochronology and tectonic units of the basement complex of northeast Africa". Proc. R. Soc. Lond., Ser. A, 350. 1976. pp. 127-141, London.

[15] C. R. Neary, I. G. Gass, and B. J. Cavanagh, "Granitic association of northeastern Sudan". Bull. Geol. Soc. Am., 87. 1976. pp.1501 -1512, Baltimore.

[16] E. M. Abdel Rahman, "Geochemical and geotectonic controls of the metallogenic evolution of selected ophiolite complexes from the Sudan". Berliner geowissenschaftliche Abhandlungen, 145. 1993.

[17] A. Kröner, R. Greiling, T. Reischmann, I. M. Hussein, R. J. Stern, S. Dürr, R. Kruger, and M. Zimmer, "Pan-African crustal evolution in the Nubian segment of Northeast Africa". In: Kröner, A. (ed.). "Proterozoic Lithosphere Evolution", Geodynamics Series. International Lithosphere Program contribution. American Geophysical Union, Washington, 17, 1987. pp. 235–257.

[18] J. R. Vail, "Tectonics and evolution of the Proterozoic basement of north-eastern Africa". In: E l Gaby, S. and Grei1ing, R. 0. (eds.) "The Pan-African Belt of Northeast Africa and adjacent areas". F. Vieweg: Braunschweig. 1988. pp. 195-226.

[19] A. A. Ahmed, "General outline of the geology and Mineral occurrences of the Red Sea Hills". Bull. Geol. Miner. Resour. Sudan, 30. 1979. pp. 63, Khartoum.

[20] P. R. Johnson, M. G. Abdelsalam, and R. J. Stern, "The Bi'r Umq-Nakasib suture in the Arabian–Nubian Shield: a key to understanding crustal growth in the East African Orogen". Gondwana Research. 6. 2003. pp. 523–530.

[21] B. Blasband, B. "Neoproterozoic Tectonics of the Arabian-Nubian Shield". Ph. D. Thesis, Utrecht University. Netherlands. http://www.geo.uu.nl/. 2006.

[22] M. J. Abram, D. Brown, L. Lepley, and R. Sadowski, "Remote sensing of porphyry copper deposits in Southern Arizona. Econ. Geol. 78. 1983. pp. 591–604.

[23] F. F. Sabin, "Remote Sensing for Mineral Exploration. Ore Geology Reviews, 14. 2000. pp 157-183, Elsevier.